AMERICAN SOCIETY FOR MICROBIOLOGY | Journal of Bacteriology®

RESEARCH ARTICLE

Genetic Evidence for Signal Transduction within the *Bacillus subtilis* GerA Germinant Receptor

Jeremy D. Amon,[a] Lior Artzi,[a] David Z. Rudner[a]

[a]Department of Microbiology, Harvard Medical School, Boston, Massachusetts, USA

ABSTRACT Bacterial spores can rapidly exit dormancy through the process of germination. This process begins with the activation of nutrient receptors embedded in the spore membrane. The prototypical germinant receptor in *Bacillus subtilis* responds to L-alanine and is thought to be a complex of proteins encoded by the genes in the *gerA* operon: *gerAA*, *gerAB*, and *gerAC*. The GerAB subunit has recently been shown to function as the nutrient sensor, but beyond contributing to complex stability, no additional functions have been attributed to the other two subunits. Here, we investigate the role of GerAA. We resurrect a previously characterized allele of *gerA* (termed *gerA**) that carries a mutation in *gerAA* and show that it constitutively activates germination even in the presence of a wild-type copy of *gerA*. Using an enrichment strategy to screen for suppressors of *gerA**, we identified mutations in all three *gerA* genes that restore a functional receptor. Characterization of two distinct *gerAB* suppressors revealed that one (*gerAB[E105K]*) reduces the GerA complex's ability to respond to L-alanine, while another (*gerAB[F259S]*) disrupts the germinant signal downstream of L-alanine recognition. These data argue against models in which GerAA is directly or indirectly involved in germinant sensing. Rather, our data suggest that GerAA is responsible for transducing the nutrient signal sensed by GerAB. While the steps downstream of *gerAA* have yet to be uncovered, these results validate the use of a dominant-negative genetic approach in elucidating the *gerA* signal transduction pathway.

IMPORTANCE Endospore formers are a broad group of bacteria that can enter dormancy upon starvation and exit dormancy upon sensing the return of nutrients. How dormant spores sense and respond to these nutrients is poorly understood. Here, we identify a key step in the signal transduction pathway that is activated after spores detect the amino acid L-alanine. We present a model that provides a more complete picture of this process that is critical for allowing dormant spores to germinate and resume growth.

KEYWORDS germination, sporulation, exit from dormancy, nutrient receptor

In response to nutrient deprivation, many bacterial species from the orders *Bacillales* and *Clostridiales* differentiate into metabolically dormant and highly resilient endospores (here referred to as "spores") (1, 2). Spore-forming organisms are ubiquitous in the environment and include many medically, agriculturally, and technologically important species. These include the causative agents of anthrax and tetanus, the pesticide-producing *Bacillus thurengiensis*, and *Bacillus cereus*, an agent of foodborne illness (3, 4). Spores have the remarkable ability to resist biological, chemical, and physical assaults and can remain dormant for decades (3, 5). Despite this ability to remain inert under extreme conditions, they can rapidly exit dormancy upon exposure to specific nutrients through a process called germination (6, 7).

Germination relies on a finely tuned mechanism of environmental sensing and subsequent response. The process is initiated by germinant receptors embedded in the spore inner membrane, which are triggered by a range of small molecules, including amino acids, nucleosides, and sugars (8). In *Bacillus subtilis*, the prototypical germinant receptor is encoded by the genes of the *gerA* operon—*gerAA*, *gerAB*, and *gerAC*—and can induce germination in response to L-alanine (9–11). Recent work has established that nutrient sensing involves

Editor Tina M. Henkin, Ohio State University

Address correspondence to David Z. Rudner, david_rudner@hms.harvard.edu.

The authors declare no conflict of interest.

For a commentary on this article, see https://doi.org/10.1128/jb.00579-21.

Received 13 September 2021
Accepted 6 November 2021
Accepted manuscript posted online 15 November 2021
Published 15 February 2022

a binding pocket in the core of the polytopic membrane protein GerAB (12). The roles of GerAA and GerAC in the germination pathway remain unknown. The next steps have been described physiologically, but mechanistic details remain lacking. First, monovalent ions are released. This is rapidly followed by the expulsion of large stores of the small molecule dipicolinic acid (DPA) in complex with Ca^{2+} from the spore core, allowing partial rehydration (13, 14). Next, two functionally redundant cell wall hydrolases, SleB and CwlJ, are activated and digest the specialized spore peptidoglycan, known as the cortex (15, 16). CwlJ is thought to be activated by DPA, but the precise mechanism of activation remains unclear, as does the mechanism of activation of SleB (17, 18). Degradation of the spore cortex by SleB and CwlJ allows complete rehydration of the core, resumption of metabolic processes, and outgrowth of the vegetative cell.

Misregulation of this process can be catastrophic for the organism. Indeed, any spore that is unable to germinate is essentially dead (19). Conversely, spores that germinate too readily risk emerging into a compromised environment (20). These two extremes highlight the twin therapeutic potentials of studies on germination: spores that can be prevented from germinating pose no threat, and those that can be forced to germinate can be easily treated with antibiotics. However, much remains to be understood about the germination pathway and its potential Achilles' heels before it can be exploited for medical or industrial purposes. With the L-alanine-binding pocket in GerAB now identified, the question becomes what happens next? How is the signal transduced? And what, if any, are the roles of GerAA and GerAC in information transduction?

Due to the challenges of reconstituting the GerA membrane complex *in vitro* and establishing an assay for signal transduction, these questions have gone largely unanswered. However, the presence of a receptor-ligand interaction at the head of a relatively unexplored signaling pathway is an alluring prospect for classical genetic analysis. Theoretically, constitutively active mutants of the *gerA* receptor that prematurely trigger spore germination can be exploited. Suppressors of such constitutively active mutants can be selected because they will regain their heat resistance through inhibition of *gerA*-induced germination. These suppressors have the potential to reveal steps downstream of nutrient detection.

Previously published work uncovered a potential candidate for such analysis. An allele of *gerAA*, *gerAA-113*, was found to have a single amino acid change of a proline at position 326 to serine. This mutation resulted in the production of phase-dark spores at the end of sporulation. The authors hypothesized that this phenotype was a result of the receptor being triggered spontaneously (21). Here, we resurrect *gerAA-113* and show that it is a dominant-negative hyperactive allele and thus well suited to genetic analysis. Using this allele, we identified suppressors that map to the *gerA* locus. The characterization of two *gerAB* suppressors provides evidence that GerAA is responsible for transducing the nutrient signal sensed by GerAB. We discuss these alleles in the context of an AlphaFold2-predicted structure (22, 23) of the GerA complex.

RESULTS

***gerAA(P326S)* triggers DPA release and SleB activation.** We began by characterizing the *gerAA(P326S)* allele. We reasoned that if this allele is hypermorphic, it should be dominant negative and result in phase-dark spores in a merodiploid strain carrying the native copy of *gerA*. We rebuilt the *P326S* mutation into the *gerA* operon and inserted it at an ectopic locus (*ycgO*) in the genome. For the purposes of this article, this allele, *ycgO::gerAA(P326S)-gerAB-gerAC*, is referred to as *gerA**. As can be seen in Fig. 1A, sporulating cells harboring *gerA** and the native *gerA* locus produced an abundance of phase-dark spores. Furthermore, when sporulated cultures of the *gerA*/gerA*$^+$ merodiploid were subjected to heat treatment to kill vegetative cells and heat-sensitive spores, there was a corresponding drop in spore viability to approximately 3% of wild type. Importantly, these phenotypes were not observed in a strain containing an additional copy of the wild-type *gerA* operon at the same ectopic locus. We conclude that *gerA** is a hyperactive dominant-negative allele.

Previous studies have shown that the transition of spores from phase gray to phase dark is dependent on the cell wall hydrolase SleB (24). To confirm that *gerA** was inducing

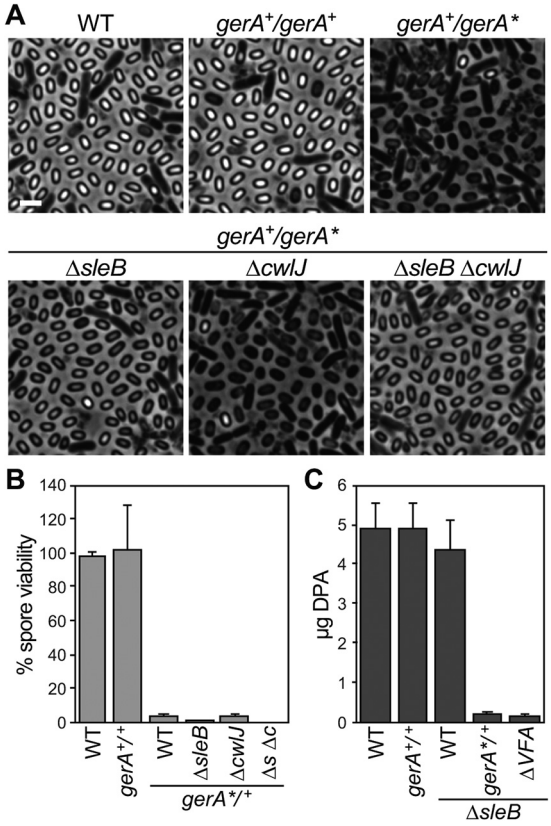

FIG 1 GerA* triggers DPA release and SleB activation. (A) Phase-contrast micrographs of the indicated strains sporulated by nutrient exhaustion for 30 h. *gerA*$^+$*/gerA*$^+$ is a merodiploid strain with two copies of the wild-type (WT) *gerA* locus. *gerA*$^+$*/gerA** is a merodiploid strain with a wild-type *gerA* locus and a mutant *gerA** operon at an ectopic genomic locus. Experiments were performed in biological triplicate; representative images are shown. Bar, 2 μm. (B) Sporulated cultures in panel A were heat treated (80°C for 20 min), and serial dilutions were plated on LB to assess heat-resistant CFU. Wild-type spore viability (3.3×10^8 CFU/mL) was set to 100%. Δ*s* Δ*c,* Δ*sleB* Δ*cwlJ*. The error bars indicate the standard deviation ($n = 3$). (C) Phase-gray and phase-bright spores were purified from sporulated cultures in panel A. Spores were boiled to release dipicolinic acid (DPA). DPA was then quantified using $TbCl_3$ compared to standards. The values are reported as micrograms of DPA released from 1 mL of purified spores adjusted to $OD_{600} = 1$. Δ*VFA*, Δ*spoVFA*. The error bars indicate the standard deviation ($n = 4$).

this transition, we analyzed the *gerA**/*gerA*$^+$ merodiploid in a Δ*sleB* background. As anticipated, this strain produced phase-gray spores instead of phase-dark spores. Furthermore, the absence of SleB in the *gerA**/*gerA*$^+$ strain caused a further drop in spore viability to approximately 0.2% of wild type. In contrast, the absence of the functionally redundant cell wall hydrolase CwlJ did not alter the phase-dark phenotype, nor did it alter spore viability. Thus, *gerA** causes premature germination in part through the activation of SleB.

The appearance of phase-gray spores is thought to reflect the failure to accumulate and retain DPA and the partial hydration of the core. To investigate whether *gerA** spores accumulate and retain DPA, we purified spores from the *gerA**/*gerA*$^+$ Δ*sleB* mutant and quantified the intracellular stores of DPA. As can be seen in Fig. 1C, wild-type, *gerA*$^+$*/gerA*$^+$, and Δ*sleB* spores contained 4 to 5 μg of DPA per 1 optical density at 600 nm (OD_{600}) equivalent. In contrast, *gerA*$^+$*/gerA** Δ*sleB* spores contained 0.24 μg. This low level was comparable to the background level detected in Δ*spoVFA* Δ*sleB* spores, which lack the DPA synthesis machinery. Altogether, these data support the idea that sporulating cells that produce GerA receptors with GerAA(P326S) trigger SleB activation and the release of DPA during spore formation.

An enrichment screen for suppressors of *gerA** identifies mutations throughout the ***gerA*** operon.** To probe the germination pathway, we sought to identify mutations that suppress the premature germination caused by *gerA**. Due to the presence of other functional germinant receptors, the most common suppressors of *gerA** were expected to be mutations

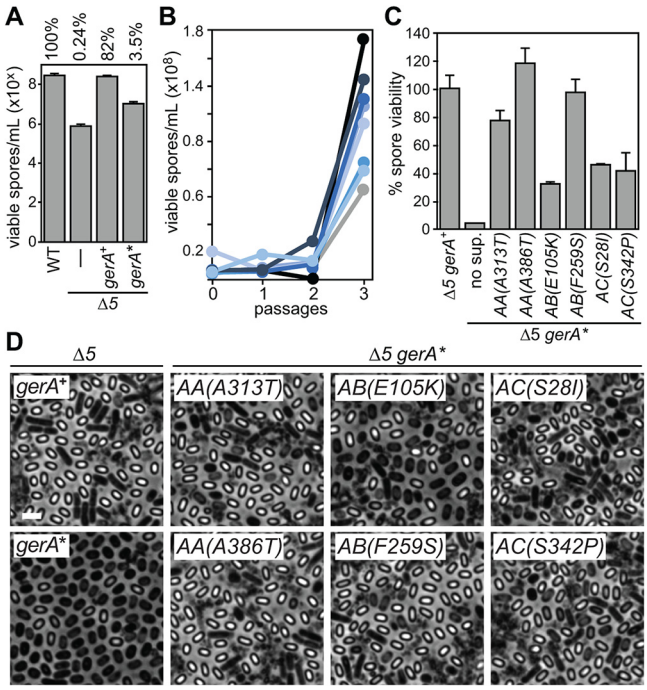

FIG 2 An enrichment screen for suppressors of *gerA**. (A) Cultures were sporulated by nutrient exhaustion and heat treated (80°C for 20 min). Serial dilutions were plated on LB to assess heat-resistant CFU. Wild-type spore viability (3.0×10^8 CFU/mL) was set to 100%. Δ*5*, Δ*gerA* Δ*gerBB* Δ*gerKB* Δ*yndE* Δ*yfkT*. The values are reported on a logarithmic scale for clarity. The error bars indicate the standard deviation ($n = 5$). (B) Cultures of Δ*5 gerA** cells were sporulated by nutrient exhaustion and heat treated. A sample was taken to assess heat-resistant CFU by plating serial dilutions on LB. Another sample of ~10^6 viable spores was then used to inoculate fresh cultures, which allowed the spores to germinate, outgrow, and resporulate upon nutrient exhaustion. This process was repeated until spore viability increased. A sample of eight independent lineages are shown. The values are reported on a linear scale for clarity. (C) Cultures were sporulated overnight and heat treated. Serial dilutions were plated on LB to assess heat-resistant CFU. Δ5 *gerA*$^+$ spore viability (2.2×10^8 CFU/mL) was set to 100%. The error bars indicate the standard deviation ($n = 3$). (D) Micrographs of sporulated cultures from panel C. Representative images from three biological replicates are shown. Bar, 2 μm.

that inactivate *gerAA*(P326S). Accordingly, to select for informative suppressors of *gerA**, we deleted the native *gerA* locus and the operons encoding the other four Ger receptors (*gerB*, *gerK*, *yfk*, and *ynd*). This strain, referred to as Δ*5*, is unable to respond to germinants, with a resultant spore viability of 0.24% of wild type (Fig. 2A). Importantly, an ectopic copy of the wild-type *gerA* locus can complement the Δ*5* strain, restoring spore viability to 82%. In contrast, spore viability of the Δ*5* strain harboring *gerA** was 3.5%. As anticipated, *gerA** continued to inappropriately cause DPA release and SleB activation when it was the sole germinant receptor (Fig. S1). The Δ*5* strain therefore creates a restrictive genetic background. Suppressors of Δ*5 gerA** cannot simply inactivate *gerA**, or else they would be unable to germinate. Rather, suppressors must maintain function while abrogating premature activation.

To select for suppressors of Δ*5 gerA**, we used a serial enrichment strategy. Overnight sporulation cultures were heat treated to kill vegetative cells and prematurely germinated spores. A sample of the culture was taken to monitor spore viability by plating for CFU. Approximately 10^6 viable, heat-resistant spores were then used to inoculate fresh sporulation medium. This process was repeated until suppressors overtook the culture and resulted in an increase in viable spores, which almost always occurred after the third passage (Fig. 2B). Cultures were then streak purified, and individual colonies were screened for the suppressive phenotype.

In total, 83 suppressors of Δ*5 gerA** were identified and further characterized. We began by backcrossing the *gerA** locus into the Δ5 mutant to determine whether the suppressors were linked to *gerA**. Strikingly, all 83 suppressors mapped to the *gerA** locus. In total, 46 unique mutations were identified in 38 codons spanning all three

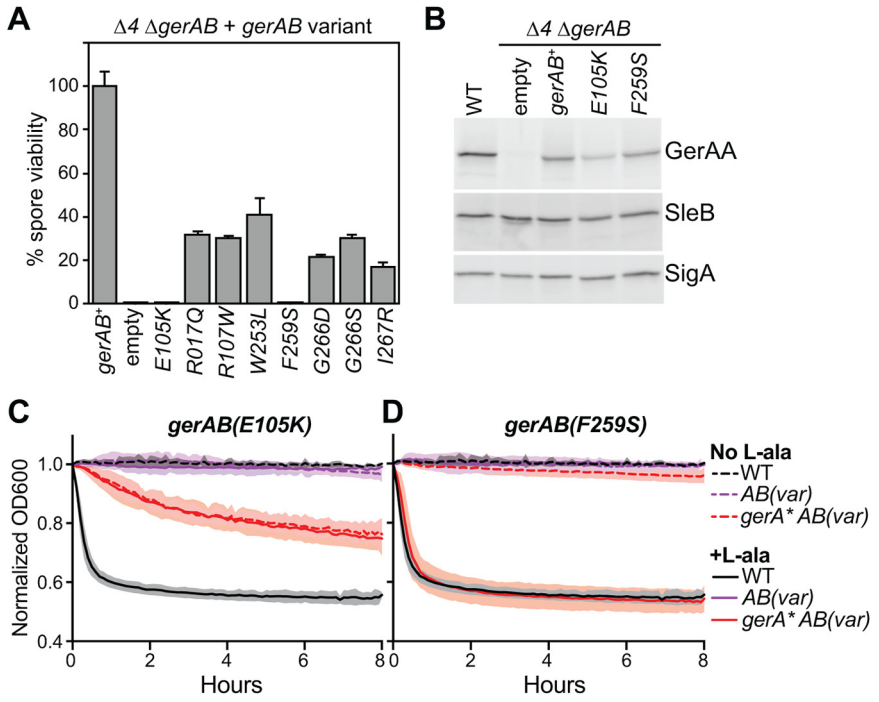

FIG 3 Analysis of GerAB suppressor mutants. (A) The indicated strains were sporulated overnight and heat treated. Serial dilutions were plated on LB to assess heat-resistant CFU. Δ*4,* Δ*gerBB* Δ*gerKB* Δ*yndE* Δ*yfkT*. *gerAB*$^+$ spore viability (3.5×10^8 CFU/mL) was set to 100%. The error bars indicate the standard deviation (n = 3). (B) Immunoblots of *gerAB* variants. Cultures were sporulated overnight. Phase-gray and phase-bright spores were purified using lysozyme and SDS. The spores were physically disrupted, and lysates were subjected to SDS-PAGE followed by immunoblot analysis to detect the presence of GerAA. SleB and SigA were analyzed to control for loading. Representative immunoblots are shown (n = 3). (C, D) Germination of *gerAB* variants. Cultures were sporulated overnight, and phase-bright spores were purified using density gradients. Spores were resuspended in 96-well plates in the presence or absence of L-alanine and agitated for 8 h at 37°C. Optical density at time zero was normalized to 1, and subsequent measurements were taken every 2 min. The shaded area indicates the standard deviation of three biological replicates. *AB(var)* indicates *gerAB (E105K)* or *gerAB(F259S)* in panel C or D, respectively. Note that the solid purple, dotted purple, and dotted black lines are superimposed. OD_{600}, optical density at 600 nm.

genes in the operon (Table S1). Fig. 2C shows the spore viability of six representative suppressors within *gerAA*, *gerAB*, and *gerAC*, with suppression of the *gerA** allele causing an increase in spore viability ranging from 10- to 30-fold. Phase-contrast microscopy of overnight sporulating cultures confirmed suppression of premature germination, with the proportion of phase-bright spores increasing as suppression improved (Fig. 2D).

***gerAB* mutants attenuate the germination signal upstream of *gerA**.** Recent studies have established an L-alanine-binding pocket in the core of the GerAB protein (12). The existence of *gerA** suppressors in *gerAB* presented a possibility to investigate how the GerAA subunit is linked to the binding pocket. In one model, *gerAA* plays a purely structural role and stabilizes the complex. In another, *gerAA* acts "upstream" of L-alanine binding, either by controlling access to the binding pocket or shaping the binding pocket to tune specificity or affinity. In a third model, *gerAA* acts "downstream" of L-alanine binding, transducing and/or processing the signal and passing this information to other parts of the complex or to other proteins.

To explore these models, we rebuilt our *gerAB* suppressor mutations and introduced them at an ectopic genomic locus in a strain that lacked *gerAB* and contained inactivating alleles of *gerB*, *gerK*, *yfk*, and *ynd* (Δ*4* Δ*gerAB*). As seen in Fig. 3A, a wild-type copy of *gerAB* inserted at the ectopic locus complemented the Δ*4* Δ*gerAB* strain. The absence of a complementing allele phenocopied the Δ*5* strain, with spore viability at 0.2% of wild type. Six *gerAB* suppressors (*R107Q*, *R107W*, *W253L*, *G266D*, *G266S*, and *I267R*) inserted at the same ectopic locus partially complemented the Δ*4* Δ*gerAB* strain, with spore viability restored to 15 to

40% of wild type. One possible explanation for why hypomorphic *gerAB* mutants suppress *gerAA(P326S)* is that the hyperactive GerA* receptor complex can respond to low levels of L-alanine present during sporulation. This concentration is not sufficient to induce germination of wild-type GerA but can further stimulate germination of GerA*. In this context, hypomorphic *gerAB* alleles suppress *gerA** by dampening this response.

In addition to the hypomorphic alleles, we identified two *gerAB* suppressors (E105K and F259S) that failed to complement the Δ*4* Δ*gerAB* mutant, with spore viability of 0.2%. This loss-of-function phenotype was not due to destabilization of the germination complex, as the levels of GerAA in spores derived from both mutants were similar, or nearly so, to spores harboring a wild-type *gerAB* allele (Fig. 3B). These levels of GerAA have been previously shown to support efficient spore germination (12). To directly assess germination in these GerAB mutants, we purified phase-bright spores and monitored germination kinetics after the addition of L-alanine. As previously shown, wild-type spores are stable in the absence of nutrients but germinate within 30 min after the addition of 1 mM L-alanine, as assayed by a drop in optical density (25). As anticipated, Δ*4* Δ*gerAB* strains harboring either *gerAB(E105K)* or *gerAB(F259S)* were stable over 8 h and were unresponsive to the addition of L-alanine (Fig. 3A and B). Collectively, these data indicate that *gerAB(E105K)* and *gerAB(F259S)* are stable, null alleles of *gerAB*.

The fact that these *gerAB* null alleles were able to form viable spores when combined with *gerAA(P326S)* led us to hypothesize that *gerAA* acts downstream of *gerAB*. To characterize this genetic interaction further, we purified phase-bright spores from the *gerAB* mutants in the *gerA** background. Interestingly, the *gerAB(E105K) gerA** spores germinated slowly but steadily over 8 h in the absence of L-alanine (Fig. 3C). Microscopic examination of the purified spores over this 8-h period confirmed this spontaneous germination and transition to phase-dark spores without the addition of L-alanine (Fig. S2). Importantly, the addition of L-alanine did not change the germination rate of these spores. These data indicate that *gerAB (E105K)* is unresponsive to L-alanine and that *gerAA(P326S)* bypasses this defect by germinating in a constitutive, ligand-independent manner.

Similarly, purified spores carrying *gerAA(P326S)* in combination with *gerAB(F259S)* germinated in the absence of L-alanine, albeit very slowly (Fig. 3D). Phase-contrast microscopy confirmed this subtle phenotype, revealing a subset of spores that had spontaneously germinated in the absence of L-alanine (Fig. S2). However, in contrast to *gerAB(E105K)*, spores carrying *gerAA(P326S)* and *gerAB(F259S)* are responsive to L-alanine, germinating as rapidly and fully as WT. We conclude that GerAB(F259S) is responsive to L-alanine but somehow dampens the signal to the point of loss-of-function. However, in the presence of GerAA(P326S), the dampened signal is restored, leading to a wild-type germination response.

***gerAB(F259S)* blocks germination signal emanating from the GerAB binding pocket.** To further explore whether the F259S substitution in GerAB dampens the nutrient signal emanating from the binding pocket, we turned to other hyperactive *gerA* alleles. A recent study found that mutating key binding pocket residues in *gerAB* can mimic L-alanine binding and result in premature germination (12). One such allele, *gerAB(T287L)*, produces phase-dark spores and results in 21% spore viability because of increased heat sensitivity. To test whether the F259S substitution could dampen the premature germination signal resulting from *gerAB(T287L)*, we combined the two mutations in *gerAB* and tested spore viability. We found that F259S prevented premature germination triggered by the T287L substitution, producing phase-bright spores (Fig. 4). Furthermore, consistent with *F259S* being downstream of *T287L*, we found that spore viability of the *gerAB(F259S,T287L)* double mutant phenocopied the *gerAB(F259S)* substitution, with 0.17% spore viability. The phase-bright phenotype in combination with low spore viability is consistent with the spores being unable to germinate. This contrasts with the interaction between *gerAA(P326S)* and *gerAB (F259S)*, which results in 97% spore viability (Fig. 2C). Similar results were found when analyzing another allele that activates germination by mimicking L-alanine binding, *gerAB(V101F)* (Fig. S3). Taken together, we conclude that the *gerAB(F259S)* mutant uncovers a step downstream of nutrient sensing in the spore germination pathway.

AlphaFold-predicted structure of the GerA complex reveals a putative signal transduction domain. The *gerAA(P326S)* and *gerAB(F259S)* variants are mutually suppressive and together restore the wild-type L-alanine response. This led us to consider the possibility

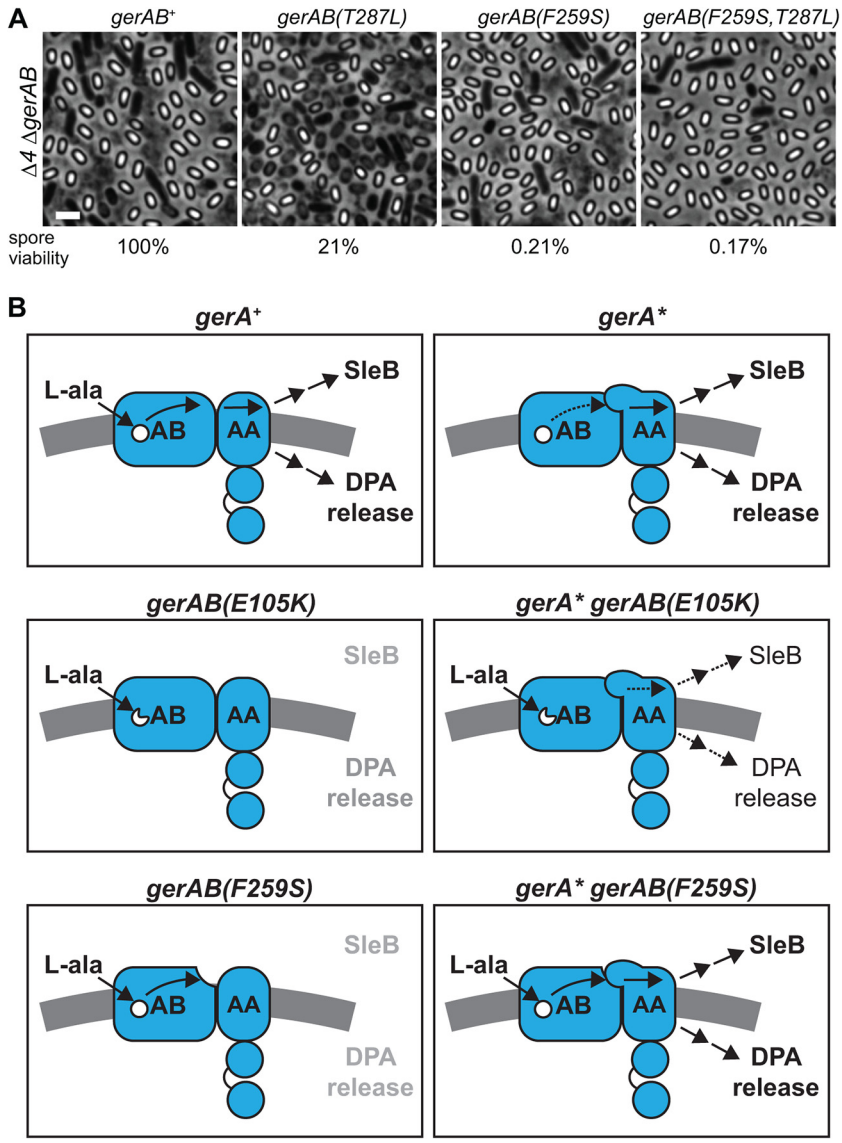

FIG 4 Epistatic analysis of *gerAB(F259S)* and *gerAB(T287L)*. (A) Cultures were sporulated by nutrient exhaustion. Representative phase-contrast micrographs of three biological replicates are shown. Bar, 2 μm. The cultures were heat treated (80°C for 20 min), serially diluted, and plated on LB to assess heat-resistant CFU. *gerAB*$^+$ spore viability (3.7×10^8 CFU/mL) was set to 100%. (B) Model of signal transduction within the GerA complex. GerAC has been omitted for clarity.

that the two mutations alter a contact point between GerAA and GerAB. To explore physical interactions between GerAA and GerAB, we assembled a predicted structure of the GerA complex using AlphaFold2.0 (22, 23). The AlphaFold algorithm predicts that GerA forms a complex (Fig. S4A). GerAA and GerAB are predicted to lie adjacent to one another, with transmembrane helix four of GerAB predicted to be in direct contact with the sixth transmembrane helix of GerAA (Fig. 5A). Furthermore, GerAC is predicted to contact both GerAA and GerAB on their extracellular surfaces.

In addition to these contacts, the algorithm predicted that the first extracellular loop of GerAA and the fourth extracellular loop of GerAB are in proximity. On GerAA, this extracellular loop consists of a short helix oriented perpendicularly to the transmembrane helices (Fig. 5B). Residue P326 of GerAA is predicted to be an anchor point of this loop. Interestingly, 27 of the 58 independently isolated suppressors that mapped to *gerAA* were found on this extracellular loop or its anchor points, suggesting that stabilizing this loop may be critical to restoring GerAA function (Table S1). On GerAB, extracellular loop four is a

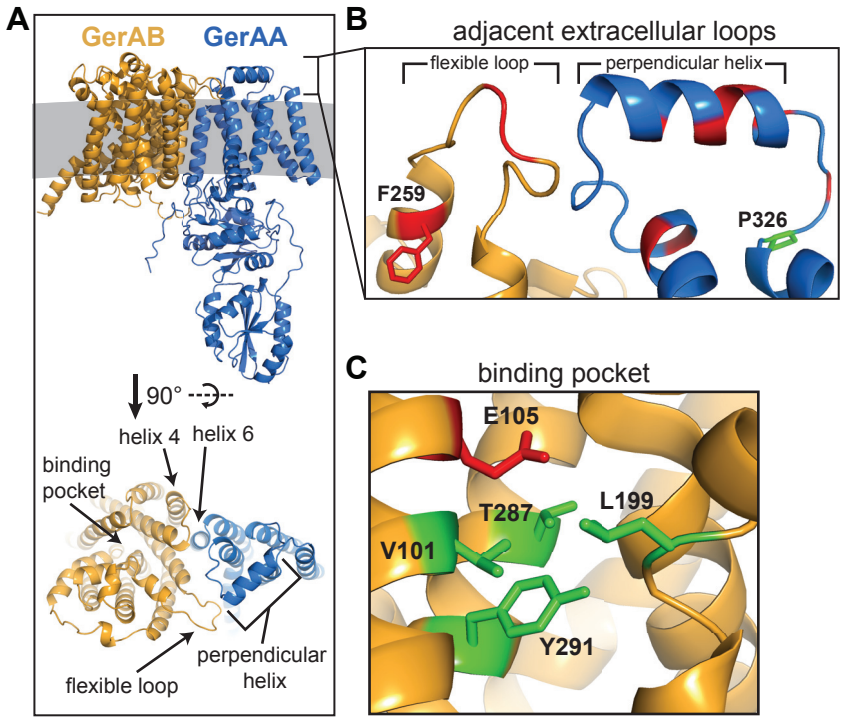

FIG 5 Predicted structures of GerAA and GerAB. (A) The top panel shows Alphafold2-predicted structures of GerAA and GerAB in complex, situated in the inner spore membrane (gray). The bottom panel shows the predicted structures rotated 90° for a top-down view. Helix 4 of GerAB and helix 6 of GerAA are predicted to form a contact interface between the two proteins. The binding pocket of GerAB is visible, as is the proximity of the flexible loop in GerAB and the perpendicular helix in GerAA. (B) View of the predicted interface between the flexible loop of GerAB and the perpendicular helix of GerAA. Residue F259 of GerAB is shown in red, and residue P326 of GerAA is shown in green. Other residues that, when mutated, were able to suppress *gerAA(P326S)* are highlighted in red. (C) View of the L-alanine-binding pocket in GerAB. Residue E105 is shown in red. Residues that have been previously shown to constitute the binding pocket (V101, T287, L199, and Y291) are shown in green (12).

region of low confidence, as measured by predicted local distance difference test (plDDT), indicating that this loop may be flexible or unstructured (Fig. S4C). Residue F259 of GerAB is predicted to be at an anchor point of this loop. Of the 19 independently isolated suppressors that mapped to *gerAB*, 12 were found on this flexible loop or its anchor points, indicating that this loop may also be critical to restoring GerAA function (Fig. 5B). These findings raise the possibility that an interaction between these extracellular loops could serve to transduce the germination signal emanating from the binding pocket in GerAB.

Lastly, to better understand how *gerAB(E105K)* was affecting nutrient detection, we analyzed the L-alanine-binding pocket of GerAB. Residue E105 is predicted to be in close proximity to the four residues that have been previously shown to constitute the GerAB binding pocket (V101, L199, T287, and Y291). The predicted structure suggests that GerAB (E105K) is unresponsive to L-alanine because it either distorts the binding pocket or prevents it from transmitting signal to the rest of the complex.

DISCUSSION

We have shown that *gerAA(P326S)* inappropriately activates germination by triggering both DPA release and SleB activation. We selected for suppressors of this allele and found 46 unique mutations in the *gerA* operon. Of these mutations, 10 mapped to *gerAB*, two of which were of particular interest. The first, *gerAB(E105K)*, failed to germinate in response to L-alanine. In combination with *gerAA(P326S)*, *gerAB(E105K)* remained unresponsive to L-alanine and germinated constitutively at a lower rate than *gerAA(P326S)* itself. Position E105 is predicted to be near the binding pocket in the core of GerAB. The second suppressor of interest, *gerAB(F259S)*, also failed to germinate in response to L-alanine and furthermore

could inhibit premature germination induced by mutations in the nutrient binding pocket. In combination with *gerAA(P326S)*, *gerAB(F259S)* regained its responsiveness to L-alanine and germinated constitutively, albeit at a very low rate. Position F259 is predicted to be at the base of a flexible, extracellular loop of GerAB.

Taken together, these results inform a model of signal transduction within the GerA receptor complex (Fig. 4B). In the wild-type case, the complex is in the "off" state yet poised to respond. When L-alanine binds the pocket in the core of GerAB, a signal is transduced to the extracellular junction between GerAB and GerAA. GerAA then somehow transduces this signal to activate SleB and release DPA. When *gerAA(P326S)* is present, the extracellular junction between GerAB and GerAA is hypersensitive to signal from the binding pocket, and low levels of L-alanine in the sporangia are enough to push the complex into the "on" state. Inhibiting nutrient recognition, as with *gerAB(E105K)*, reveals the baseline constitutive activity of the *gerAA(P326S)* allele. In contrast, dampening the hyperactive extracellular junction, as with *gerAB(F259S)*, reverts the region to near-wild type, allowing the GerA complex to largely remain off yet responsive to L-alanine. When *gerAB(E105K)* or *gerAB(F259S)* are present individually, they shut down GerA completely, the first by inactivating the binding pocket and the second by dampening the extracellular junction to the point of preventing signal transduction.

Previous studies have presented evidence that GerA is likely poised on a knife's edge to respond to L-alanine (24, 26). This allows GerA to respond quickly to germinant but results in a sizable fraction of wild-type spores that will prematurely germinate due to low levels of L-alanine in the sporangia. Our analysis of *gerAA(P326S)* supports this model and offers two mechanistic explanations for how GerA has tuned its sensitivity. One, as previously shown, is by the more direct method of altering the binding pocket. The other is by changing the nature of the interaction between the extracellular loops of GerAA and GerAB. Interestingly, the studies mentioned above found that other germinant receptors, GerB and GerK, played no role in premature germination. This could be due to lower levels of GerB- and GerK-specific germinants in the sporangia or due to different sensitivities of the receptors. Analyses of the interacting extracellular region in other germinant receptors could elucidate how spores set their sensitivities to changes in their environments.

The mechanism by which *gerAA* activates downstream events remains unknown. However, the presence of a cluster of mutants predicted to reside on the extracellular region of GerAA most distal to GerAB raises the possibility that the germination signal culminates in an event at this location (GerAA residues V369, E370, and A371). One possibility is that this position is an interaction domain with another factor. Alternatively, this region could be the site of a GerAA-dependent alteration of some physical property of the spore. In the context of this model, either would in turn trigger DPA release and SleB hydrolase activation.

Selecting against two physical changes induced by germination—DPA release and SleB activation—resulted in mutants that suppress both changes simultaneously. The fact that all 83 suppressors of *gerA** were in the *gerA* operon suggests that there are no protein factors downstream of GerA capable of triggering both physical changes. For example, these data argue that the *spoVA* locus, which has been implicated in DPA release, is unlikely to also function in SleB activation (27–29). Given these 83 suppressors, if we consider mutations within the *gerA* operon and external to the *gerA* operon as binary outcomes, the genetics argue with $>$98% confidence that finding such a protein factor downstream of GerA has less than 1 in 20 odds.

This presents us with two possible models. First, that the GerA complex directly releases DPA and activates SleB. We consider this model unlikely, because members of the *spoVA* locus are likely involved in DPA release (27–29). In an alternative model, the GerA complex is a branch point between DPA release and SleB activation. With this model, suppressors of downstream events were not found because of the improbability of simultaneously selecting for two independent mutations. We favor this second model because it allows for the inclusion of *spoVA*, but further investigation is required. Our screen has validated the use of a dominant-negative genetic approach for investigating GerA, and future studies will use similar screens to clarify between the two potential models described above.

MATERIALS AND METHODS

General methods. All *B. subtilis* strains were derived from the auxotrophic (*trpC2*) strain 168 (30). To obtain spores, sporulation was induced by nutrient exhaustion. The cells were grown in liquid Difco sporulation medium (DSM) at 37°C with agitation for 24 to 30 h. Alternatively, the cells were grown on solid DSM agar at 37°C for 96 h. Spore viability was determined by comparing the total number of heat-resistant (80°C for 20 min) CFU as a percentage of wild-type heat-resistant CFU. Deletion mutants were derived from the *Bacillus* knockout (BKE) collection (31) or were generated by isothermal assembly of PCR products (32) followed by direct transformation into *B. subtilis*. All BKE mutants were backcrossed twice into *B. subtilis* 168 before assaying and prior to antibiotic cassette removal. Antibiotic cassette removal was performed using a temperature-sensitive plasmid that constitutively expresses Cre recombinase (33). All strains were constructed using a one-step competence method. Tables of strains, plasmids, and primers used in this study can be found in the supplemental information.

Genetic screen details. Fresh colonies of BJA177a (Δ*5 gerA**) were suspended in 3 mL DSM and incubated at 37°C for 24 h with agitation. The Cultures were heat treated at 80°C for 20 min. For dilutions and CFU plating, 100 μl were removed. An additional 100 μl ($\sim 10^6$ viable spores) were removed and used to inoculate fresh 3-mL DSM cultures. This process was repeated until spore viability had appreciably increased, indicating that suppressors had overtaken the cultures. These cultures were genetically heterogeneous and so were streak purified. Individual colonies were screened for retention of markers and the suppressive phenotype of increased spore viability. Genomic DNA was extracted and used to transform the *gerA** locus into the parental Δ*5* background. All backcrossed mutants retained the suppressive phenotype, indicating linkage to *gerA**. The *gerA** locus was subjected to PCR followed by Sanger sequencing to determine mutations.

Spore purification with lysozyme and SDS. A 25-mL overnight DSM culture was collected and washed three times with sterile water. Spores were resuspended in phosphate-buffered saline (PBS) containing lysozyme at a concentration of 1.5 mg/mL. The spores were then incubated at 37°C with agitation for 1 h. SDS was added to a final concentration of 2% (wt/vol), and spores were incubated for an additional 30 min at 37°C with agitation. Spores were then washed five times with water to remove the SDS.

Spores purified with density gradient. A 25-mL overnight DSM culture was heat treated (80°C for 20 min) and washed three times with sterile water. The spore pellet was resuspended in 1 mL of 20% (wt/vol) Histodenz (Sigma) and incubated for 30 min on ice. This suspension was then gently pipetted on top of 2 mL of 40% (wt/vol) Histodenz, which itself was layered on 6 mL of 50% (wt/vol) Histodenz. The gradient was centrifuged at 4,000 rpm for 90 min at 4°C, and the supernatant, which contained phase-dark spores, vegetative cells, and cell debris, was siphoned off. The pellet was washed three times with sterile water. Pellets were suspended in 1 mL H_2O and kept at 4°C All spore preparations were evaluated by phase-contrast microscopy and contained >99% phase-bright spores.

Microscopy. Overnight sporulation cultures and purified spores were concentrated by centrifugation and then immobilized on pads made of 2% (wt/vol) agarose in PBS. Phase-contrast microscopy was performed using a Nikon TE2000 inverted microscope, Nikon Intensilight Metal Halide Illumination, a Photometrics CoolSNAP HQ2 monochrome CCD camera, and a Plan Apo 100×/1.4 oil Ph3 DM objective. All exposure times were 250 ms. Image acquisition was performed using Nikon-Elements acquisition software AR 3.2. Image analysis and processing were performed in Metamorph.

SDS-PAGE and immunoblotting. The spores were purified with lysozyme and SDS and then suspended in 0.4 mL PBS with protease inhibitors. Spore resuspensions were added to 2-mL tubes containing Lysing Matrix B (MP Biomedicals, Irvine, CA) and chilled on ice. The spores were then ruptured mechanically using FastPrep (MP Biomedicals) at 6.5 m/s for 1 min. Immediately, 0.4 mL of 2× Laemmli sample buffer with 10% (vol/vol) β-mercaptoethanol was added, and the tubes were vortexed. The samples were then incubated at 80°C for 5 min and centrifuged at maximum speed for 10 min. Supernatants were collected, and the total protein was normalized using the noninterfering protein assay (G-Biosciences, St. Louis, MO).

All samples were separated by SDS-PAGE on 17.5% resolving gels, electroblotted onto Immobilon-P membranes (Millipore, Burlington, MA), and blocked in 5% nonfat milk in PBS with 0.5% Tween 20. The membranes were then probed with anti-GerAA (1:5,000) (34), anti-SigA (1:10,000) (35), or anti-SleB (1:5,000) (36) diluted in 3% BSA in PBS with 0.05% Tween 20. Primary antibodies were detected using horseradish-peroxidase conjugated anti-rabbit antibodies (Bio-Rad) and detected with Western Lightning ECL reagents.

Measuring DPA levels. The spores were purified using lysozyme and SDS and resuspended to OD_{600} = 1 in water. Spore suspensions were then incubated at 100°C for 30 min to release DPA. The suspensions were subjected to centrifugation, and the supernatants were added to a solution at a final concentration of 100 μM $TbCl_3$ in 1 M sodium acetate, pH 5.6. Fluorescence was measured at 545 nm with excitation set at 272 nm. Each sample was analyzed in technical triplicate and compared to a standard curve to determine DPA concentration.

Germination assays. The spores were purified by Histodenz gradient and resuspended in 25 mM HEPES, pH 7.4, at OD_{600} = 1.2. The suspensions were heat activated for 30 min at 70°C followed by 20 min on ice. The suspensions were then transferred to a clear, 96-well, flat-bottomed tray, and either buffer (25 mM HEPES, pH 7.4) or 1 mM L-alanine in buffer (25 mM HEPES, pH 7.4) was added for a final OD_{600} = 0.6. The 96-well trays were agitated in a TECAN plate reader at 37°C, and optical density readings were taken every 2 min. The spores were tested in technical triplicate, and the values were averaged.

SUPPLEMENTAL MATERIAL

Supplemental material is available online only.

SUPPLEMENTAL FILE 1, PDF file, 9.7 MB.

ACKNOWLEDGMENTS

We thank all members of the Bernhardt-Rudner supergroup past and present for helpful advice, discussions, and encouragement. We thank Paula Montero Llopis, Ryan Stephansky, and the Harvard Medical School Microscopy Resources on the North Quad (MicRoN) core for advice on microscopy. Portions of this research were conducted on the O2 High Performance Computing Cluster, supported by the Research Computing Group, at Harvard Medical School. See https://it.hms.harvard.edu/our-services/research-computing for more information.

Support for this work comes from National Institutes of Health grants GM086466 and GM127399 and funds from the Harvard Medical School Dean's Initiative (D.Z.R.). J.D.A. was funded by National Institutes of Health grant F32GM130003. L.A. is a Simons Foundation fellow of the Life Sciences Research Foundation.

REFERENCES

1. Tan IS, Ramamurthi KS. 2014. Spore formation in *Bacillus subtilis*. Environ Microbiol Rep 6:212–225. https://doi.org/10.1111/1758-2229.12130.
2. Higgins D, Dworkin J. 2012. Recent progress in *Bacillus subtilis* sporulation. FEMS Microbiol Rev 36:131–148. https://doi.org/10.1111/j.1574-6976.2011.00310.x.
3. Setlow P. 2014. Spore resistance properties. Microbiol Spectr 2. https://doi.org/10.1128/microbiolspec.TBS-0003-2012.
4. Bottone EJ. 2010. *Bacillus cereus*, a volatile human pathogen. Clin Microbiol Rev 23:382–398. https://doi.org/10.1128/CMR.00073-09.
5. Ulrich N, Nagler K, Laue M, Cockell CS, Setlow P, Moeller R. 2018. Experimental studies addressing the longevity of *Bacillus subtilis* spores – The first data from a 500-year experiment. PLoS One 13:e0208425. https://doi.org/10.1371/journal.pone.0208425.
6. Setlow P, Wang S, Li YQ. 2017. Germination of spores of the orders Bacillales and Clostridiales. Annu Rev Microbiol 71:459–477. https://doi.org/10.1146/annurev-micro-090816-093558.
7. Moir A, Cooper G. 2015. Spore germination. Microbiol Spectr 3. https://doi.org/10.1128/microbiolspec.TBS-0014-2012.
8. Ross C, Abel-Santos E. 2010. The Ger receptor family from sporulating bacteria. Curr Issues Mol Biol 12:147–158. https://doi.org/10.21775/cimb.012.147.
9. Moir A, Lafferty E, Smith DA. 1979. Genetics analysis of spore germination mutants of *Bacillus subtilis* 168: the correlation of phenotype with map location. J Gen Microbiol 111:165–180. https://doi.org/10.1099/00221287-111-1-165.
10. Paidhungat M, Setlow P. 1999. Isolation and characterization of mutations in *Bacillus subtilis* that allow spore germination in the novel germinant D-alanine. J Bacteriol 181:3341–3350. https://doi.org/10.1128/JB.181.11.3341-3350.1999.
11. Paidhungat M, Setlow P. 2000. Role of Ger proteins in nutrient and nonnutrient triggering of spore germination in *Bacillus subtilis*. J Bacteriol 182:2513–2519. https://doi.org/10.1128/JB.182.9.2513-2519.2000.
12. Lior A, Assaf A, Kelly PB, Anna GG, Amy T, Fernando HR-G, Debora M, Andrew K, David ZR. 2021. Dormant spores sense amino acids through the B subunits of their germination receptors. bioRxiv. https://doi.org/2021.10.28.466322.
13. Swerdlow BM, Setlow B, Setlow P. 1981. Levels of H^+ and other monovalent cations in dormant and germinating spores of *Bacillus megaterium*. J Bacteriol 148:20–29. https://doi.org/10.1128/jb.148.1.20-29.1981.
14. Paidhungat M, Setlow B, Driks A, Setlow P. 2000. Characterization of spores of *Bacillus subtilis* which lack dipicolinic acid. J Bacteriol 182:5505–5512. https://doi.org/10.1128/JB.182.19.5505-5512.2000.
15. Popham DL, Helin J, Costello CE, Setlow P. 1996. Analysis of the peptidoglycan structure of *Bacillus subtilis* endospores. J Bacteriol 178:6451–6458. https://doi.org/10.1128/jb.178.22.6451-6458.1996.
16. Popham DL, Bernhards CB. 2015. Spore peptidoglycan. Microbiol Spectr 3:157–177. https://doi.org/10.1128/microbiolspec.TBS-0005-2012.
17. Paidhungat M, Ragkousi K, Setlow P. 2001. Genetic requirements for induction of germination of spores of *Bacillus subtilis* by Ca^{2+}-dipicolinate. J Bacteriol 183:4886–4893. https://doi.org/10.1128/jb.183.16.4886. https://doi.org/10.1128/JB.183.16.4886-4893.2001.
18. Moriyama R, Hattori A, Miyata S, Kudoh S, Makino S. 1996. A gene (sleB) encoding a spore cortex-lytic enzyme from *Bacillus subtilis* and response of the enzyme to L-alanine-mediated germination. J Bacteriol 178:6059–6063. https://doi.org/10.1128/jb.178.20.6059-6063.1996.
19. Setlow B, Melly E, Setlow P. 2001. Properties of spores of *Bacillus subtilis* blocked at an intermediate stage in spore germination. J Bacteriol 183:4894–4899. https://doi.org/10.1128/JB.183.16.4894-4899.2001.
20. Setlow P. 2006. Spores of *Bacillus subtilis*: their resistance to and killing by radiation, heat and chemicals. J Appl Microbiol 101:514–525. https://doi.org/10.1111/j.1365-2672.2005.02736.x.
21. Mongkolthanaruk W, Cooper GR, Mawer JSP, Allan RN, Moir A. 2011. Effect of amino acid substitutions in the GerAA protein on the function of the alanine-responsive germinant receptor of *Bacillus subtilis* spores. J Bacteriol 193:2268–2275. https://doi.org/10.1128/JB.01398-10.
22. Jumper J, Evans R, Pritzel A, Green T, Figurnov M, Ronneberger O, Tunyasuvunakool K, Bates R, Žídek A, Potapenko A, Bridgland A, Meyer C, Kohl SAA, Ballard AJ, Cowie A, Romera-Paredes B, Nikolov S, Jain R, Adler J, Back T, Petersen S, Reiman D, Clancy E, Zielinski M, Steinegger M, Pacholska M, Berghammer T, Bodenstein S, Silver D, Vinyals O, Senior AW, Kavukcuoglu K, Kohli P, Hassabis D. 2021. Highly accurate protein structure prediction with AlphaFold. Nature 596:583–589. https://doi.org/10.1038/s41586-021-03819-2.
23. Mirdita M, Ovchinnikov S, Steinegger M. 2021. ColabFold – Making protein folding accessible to all. bioRxiv. https://doi.org/2021.08.15.456425.
24. Ramírez-Guadiana FH, Meeske AJ, Wang X, Rodrigues CDA, Rudner DZ. 2017. The *Bacillus subtilis* germinant receptor GerA triggers premature germination in response to morphological defects during sporulation. Mol Microbiol 105:689–704. https://doi.org/10.1111/mmi.13728.
25. Keynan A, Halvorson HO. 1962. Calcium dipicolinic acid-induced germination of *Bacillus cereus* spores. J Bacteriol 83:100–105. https://doi.org/10.1128/jb.83.1.100-105.1962.
26. Grela A, Jamrożek I, Hubisz M, Iwanicki A, Hinc K, Kaźmierkiewicz R, Obuchowski M. 2018. Positions 299 and 302 of the GerAA subunit are important for function of the GerA spore germination receptor in *Bacillus subtilis*. PLoS One 13:e0198561. https://doi.org/10.1371/journal.pone.0198561.
27. Vepachedu VR, Setlow P. 2004. Analysis of the germination of spores of *Bacillus subtilis* with temperature sensitive spo mutations in the spoVA operon. FEMS Microbiol Lett 239:71–77. https://doi.org/10.1016/j.femsle.2004.08.022.
28. Perez-Valdespino A, Li Y, Setlow B, Ghosh S, Pan D, Korza G, Feeherry FE, Doona CJ, Li YQ, Hao B, Setlow P. 2014. Function of the SpoVAEa and SpoVAF proteins of *Bacillus subtilis* spores. J Bacteriol 196:2077–2088. https://doi.org/10.1128/JB.01546-14.
29. Velásquez J, Schuurman-Wolters G, Birkner JP, Abee T, Poolman B. 2014. *Bacillus subtilis* spore protein SpoVAC functions as a mechanosensitive channel. Mol Microbiol 92:813–823. https://doi.org/10.1111/mmi.12591.
30. Zeigler DR, Prágai Z, Rodriguez S, Chevreux B, Muffler A, Albert T, Bai R, Wyss M, Perkins JB. 2008. The origins of 168, W23, and other *Bacillus subtilis* legacy strains. J Bacteriol 190:6983–6995. https://doi.org/10.1128/JB.00722-08.
31. Koo B-M, Kritikos G, Farelli JD, Todor H, Tong K, Kimsey H, Wapinski I, Galardini M, Cabal A, Peters JM, Hachmann A-B, Rudner DZ, Allen KN, Typas A, Gross CA. 2017. Construction and analysis of two genome-scale deletion libraries for *Bacillus subtilis*. Cell Syst 4:291–305.e7. https://doi.org/10.1016/j.cels.2016.12.013.
32. Gibson DG. 2011. Enzymatic assembly of overlapping DNA fragments. Methods Enzymol 498:349–361. https://doi.org/10.1016/B978-0-12-385120-8.00015-2.
33. Meeske AJ, Sham L-T, Kimsey H, Koo B-M, Gross CA, Bernhardt TG, Rudner DZ. 2015. MurJ and a novel lipid II flippase are required for cell wall biogenesis

in *Bacillus subtilis*. Proc Natl Acad Sci U S A 112:6437–6442. https://doi.org/10.1073/pnas.1504967112.
34. Stewart K-AV, Yi X, Ghosh S, Setlow P. 2012. Germination protein levels and rates of germination of spores of *Bacillus subtilis* with overexpressed or deleted genes encoding germination proteins. J Bacteriol 194:3156–3164. https://doi.org/10.1128/JB.00405-12.
35. Fujita M. 2000. Temporal and selective association of multiple sigma factors with RNA polymerase during sporulation in *Bacillus subtilis*. Genes Cells 5:79–88. https://doi.org/10.1046/j.1365-2443.2000.00307.x.
36. Bernhards CB, Popham DL. 2014. Role of YpeB in cortex hydrolysis during germination of *Bacillus anthracis* spores. J Bacteriol 196:3399–3409. https://doi.org/10.1128/JB.01899-14.